Microcalorimetric Measurement of the Interactions between Water Vapor and Amorphous Pharmaceutical Solids

David Lechuga-Ballesteros,[1,3] Aziz Bakri,[2] and Danforth P. Miller[1]

Received July 26, 2002; accepted October 22, 2002

Purpose. Use a microcalorimetric technique to measure the interactions between water vapor and amorphous pharmaceutical solids and describe the relationship between long-term physical stability and the storage relative humidity (RH) at constant temperature.

Methods. A thermal activity monitor was used to characterize interactions of water vapor with spray-dried amorphous sucrose, lactose, raffinose, and sodium indomethacin. Differential scanning calorimetry was used to measure glass transition temperature, T_g. X-ray powder diffraction was used to confirm that the spray-dried samples were amorphous. Scanning electron microscopy was used to examine particle morphology. Specific surface area was determined by BET analysis of nitrogen and krypton adsorption isotherms.

Results. The moisture-induced thermal activity traces (MITATs) of the materials in this study exhibit general behavior that helps explain the effect of moisture content on the physical stability of the glassy phase at a given storage temperature. At some RH threshold, RH_m, the MITAT exhibits a dramatic increase in the energy of interaction between water vapor and the glass that cannot be explained by a phase or morphology change. Calorimetric data indicate that water vapor-solid interactions are reversible below RH_m; above RH_m, energetic hysteresis is observed and water-water interactions predominate. In addition, the MITAT was deconvoluted into sorptive and nonsorptive components, making it possible to assign the observed heat flow to unique thermal events. Samples stored at a RH just below RH_m for more than 2 months show no evidence of morphology or phase change. In addition, the MITAT can be deconvoluted into sorptive and nonsorptive components by using a twin-calorimeter arrangement. This analysis provides specificity to the microcalorimetric analysis and helps explain the nature of the physical changes that occur during the hydration glassy phase.

Conclusions. The MITAT is a useful tool to determine the onset of moisture-induced physical instability of glassy pharmaceuticals and may find a broad application to determine appropriate storage conditions to ensure long-term physical stability.

KEY WORDS: microcalorimetry; MITAT; glass transition temperature; BET monolayer; hydration limit; stability.

INTRODUCTION

Chemical reactivity or physical changes of glassy pharmaceuticals (i.e., structural collapse, crystallization) occur because of disorder and increased molecular mobility. Methods are available to estimate average relaxation times, a measure of molecular mobility, and meaningful correlations to stability have been proposed (1,2). Most techniques use the dry state (i.e., zero water content) as the reference state and therefore do not provide information on the effect of water content on average relaxation times. To our knowledge, there are only two cases in which the effect of absorbed water on the glass transition temperature, T_g, and average relaxation times has been studied (3,4). Andronis and Zografi (4) report that molecular mobility, determined from either the heating rate dependence of T_g or dielectric measurements of the average relaxation time, is significant below T_g. This helps explain why amorphous indomethacin crystallizes at temperatures well below its T_g. Kajiwara *et al.* (3) report the decrease in the "zero mobility temperature" T_o, of raffinose, measured by the heating rate dependence of T_g. However, neither of these studies addresses the relationship between T_o and a critical water content.

Water molecules are always mobile within a hydrated glassy solid. In fact, it has been shown that the diffusivity of water molecules within a glassy matrix is finite and substantial below T_g (5). However, for small molecule glasses, amorphous polymers and proteins alike, water mobility decreases at water contents below the hydration limit, W_m (6–9). It has also been shown that the degrees of freedom of water mobility within a glass are restricted below W_m. For example, dielectric resonance spectroscopy experiments on lysozyme show that water molecules are irrotationally bound to a protein surface at such hydration levels (10). The use of W_m as a moisture threshold for stability is similar to treatments based on W_g (11), the amount of water required to depress T_g to the storage temperature of the surroundings. However, W_g is a less-rigorous criterion than W_m since instability can occur at temperatures far below T_g. Furthermore, in many instances, the T_g of formulations cannot be determined because of inherent limitations of traditional experimental methods. However, it is safe to assume that the T_g of a protein-rich formulation, even at its hydration limit, is much higher than typical storage temperatures (i.e., T_g>>40°C). This is an important consideration since it demonstrates that molecular motions implicated in the decomposition processes of protein-rich formulations at low water contents may be independent of T_g, possibly because of decoupling of water mobility and protein mobility.

The hydration limit has also been linked to the long-term chemical stability of glassy formulations. Below W_m, improved chemical stability of foodstuffs (12) and therapeutic proteins has been extensively reported (13–15). In general, freeze-dried protein formulations are more stable at lower water contents. It is generally acknowledged that the molecular mobility of water and the glassy matrix at hydration levels above W_m are among the main factors that affect overall stability.

Generally, the minimum in the rate of bimolecular reactions is found near the hydration limit (12,13,16). It has been proposed that above W_m, water-water interactions increase, thereby favoring the formation of microscopic regions of condensed water. These regions can promote chemical instability since chemical species can readily dissolve, diffuse, and react (12).

In addition to the many references to the relationship between chemical stability and the hydration limit, W_m has

[1] Nektar Therapeutics (formerly Inhale Therapeutics Systems, Inc.), 150 Industrial Road, San Carlos, California 94070.

[2] Université Joseph Fourier at Grenoble, Formulation and Process Engineering, Faculty of Pharmacy, ISERM 008.

[3] To whom correspondence should be addressed. (e-mail: dlechuga@ca.nektar.com)

0724-8741/03/0200-0308/0 © 2003 Plenum Publishing Corporation

been shown to have some physical significance. For example, microcrystalline cellulose and compressible sugar lose their direct compaction properties at water contents just below the value of W_m (17) and gelatin capsules become brittle as the water content is reduced below W_m (18). It also has been demonstrated that the diffusivity of water in PVP changes dramatically at W_m (8).

The determination of W_m thus relies on the use of an adsorption model (BET or GAB) to analyze the experimental moisture sorption isotherm. The description of an experimental approach, which offers a direct measurement of W_m and a direct correlation to physical stability, is offered in the present study. In addition, the use of isothermal microcalorimetry to describe the interactions of water vapor with common pharmaceutical amorphous solids (sodium indomethacin, lactose, raffinose, sucrose, and trehalose) is described in detail.

Although isothermal microcalorimetry is a nonspecific technique by nature, with some assumptions, the calorimetric signal can be deconvoluted into contributions due to water vapor sorption/desorption and other energetic events. The separate calorimetric signals give insight into the processes that lead to instability and the environmental conditions under which they occur.

MATERIALS AND METHODS

Materials

Sucrose, α-lactose monohydrate, trehalose dihydrate, and raffinose pentahydrate were obtained from Pfanstiehl Laboratories (Waukegan, IL, USA), all at stated purities of 99.9%. These saccharides were used without further purification. Indomethacin (1-(p-chlorobenzoyl)-5-methoxy-2-methyindole-3-acetic acid) was obtained from Sigma-Aldrich (St. Louis, MO) (USP grade). For the saccharides, aqueous solutions of 1.0 wt% solids content were prepared. A 10 wt% solution of sodium indomethacin was prepared by dissolving equimolar amounts of indomethacin and NaOH in methanol. Though this treatment likely resulted in a mixture of free acid and the sodium salt, it will be referred to hereafter simply as sodium indomethacin.

All solutions were spray-dried using a modified Büchi 190 spray-dryer. For sucrose, the (controlled) inlet and (measured) outlet air temperatures were 120°C and 60°C, respectively. For lactose, trehalose, and raffinose, the inlet and outlet air temperatures were 120°C and 80°C, respectively. Sodium indomethacin was spray-dried in a nitrogen atmosphere; the inlet and outlet gas temperatures were 120°C and 90°C, respectively. To avoid structural relaxation of the amorphous powders during spray-drying, each collector was kept cool by using a water bath. Powders were stored in a drybox and handled in a glove box at less than 1%RH at ambient temperature. X-ray powder diffraction was used to confirm that all spray-dried samples were amorphous.

Methods

Isothermal Microcalorimetry

The hydration properties of spray-dried amorphous compounds were studied using a heat-conduction isothermal microcalorimetric system, TAM (Thermal Activity Monitor, Model 2277 Thermometric AB, Järfälla, Sweden). At a given temperature, this technique measures the heat flux, P (typically measured in μW) due to all energetic events. In each experiment, a powder sample was placed into a stainless steel ampoule and connected to a Gas Pressure Controller Device (GPCD) (19) (Model 2255-120 Thermometric AB, Sweden) that accurately controls the relative humidity (RH) within the measurement ampoule (0–90 ± 0.1% RH) as a step function or a linear ramp. An empty, closed ampoule was used as a reference cell. Dry N_2 was used as carrier gas at a constant flow rate (1.48 standard cm^3/minute). The RH was controlled by splitting the total flow of the carrier gas into two streams. One stream was fed directly to the sample ampoule, (i.e., the "dry stream"), while the other ("wet") stream was fed to two successive humidification chambers. A stream of a given RH was then produced by controlling the ratio of the flow rates of the wet and dry streams. The method used here requires a mathematical correction to the RH to account for the change in mass flow rate as the nitrogen stream passes through the humidification chambers. This correction was used throughout this work even though it was at most 3% of the nominal RH value (at 25°C).

In the calorimetry experiments of this work, water vapor is presented to the amorphous solid in two ways: step mode and ramp mode. In each mode, identical experiments were performed using an empty ampoule. This background contribution was subtracted from all data reported here.

Step mode: About 10 to 15 mg of powder were placed in the measuring ampoule and dried *in situ* by flowing a dry nitrogen stream (≈0% RH) until there was no measurable thermal activity (i.e., p ranging from -1 to +1 μW). Then, the RH of the incoming gas stream, RH_{in}, was set to 5% and an exothermic heat flux ($p > 0$) response was recorded. After several hours, thermal equilibrium was reached ($p \approx 0$), and RH_{in} was then set to 0%RH and an endothermic ($p < 0$) response due to moisture desorption was observed. These sorption/desorption cycles were repeated for steps of 10%RH, 15%RH, and 20%RH.

Ramp mode: About 10 to 15 mg of powder were placed in the measuring ampoule and dried as described above. The RH was then increased in a linear ramp from 0–90%RH over the following 30 h (i.e., at 3%RH/hour). The heat flow resulting from the moisture interaction with the solid sample was measured as a function of time. Since the RH ramp rate was known, the heat flow could also be plotted as a function of inlet RH, RH_{in}. Depending on the interaction of water with the amorphous solid sample, the RH of the gas stream exiting the sample cell, RH_{out} may be less than, greater than, or equal to the RH of the incoming gas stream. In the present study, a modification previously described in the literature (20) of the ′Double Twin′ Isothermal Calorimeter (DTIC) (21,22) was used to measure RH_{out}. This was accomplished by directing the exiting gas stream from the RH-perfusion cell into a second, independent calorimeter. The custom-designed sample cell in the second calorimeter was filled with pure water, which evaporates at a rate inversely proportional to the RH of the incoming airflow, RH_{out}. Knowledge of the RH_{out}, the flow rate, and the latent heat of evaporation of water allows the calculation of the amount of water gained or lost by the sample in the RH-perfusion cell. Furthermore, by assuming that the heat of sorption is equal to the heat of condensation of water, the heat flux due to sorption/desorption of water can

be calculated. Thus, the heat flux due to all other activity (i.e., structural collapse, crystallization, etc.) can be calculated by subtracting the calculated heat flux due to water sorption/desorption from the total heat flux measured in the first calorimeter.

Modulated Differential Scanning Calorimetry

The glass transition temperature, T_g, of a given sample was measured using a differential scanning calorimeter (TA Instruments, New Castle, DE, Model 2920 Modulated DSC with a refrigerated cooling system). The sample cell was purged with dry helium at a flow rate of 40 cm^3/min. Aluminum pans were filled with 2–10 mg of powder and hermetically sealed in a dry environment (RH < 1.0%). For an open-pan modulated DSC experiment, the pan was punctured with a needle just before the run. The scans were performed at 2°C/min (modulated at 0.318°C/min) with an equilibration temperature of –30°C for 15–30 min, followed by heating to 200°C. Each reported T_g corresponds to the extrapolated onset of the transition. Water loss upon heating was measured using a thermogravimetric analyzer (Hi-Res TGA 2950, TA Instruments), using open aluminum pans at various controlled scanning rates (ranging from 5–20°C/min).

X-Ray Powder Diffraction

X-ray powder diffraction (XRPD) studies were performed using an XRD-6000 diffractometer (Shimadzu Corp., Kyoto, Japan). Samples were scanned from 3° to 40° 2θ, at 3°/min, with a step size of 0.04°2θ, using a Cu radiation source with a wavelength of 1.54Å operated at 45 kV and 30 mA. To control the RH above the powder sample, an Anton Paar TTK 450 (Graz, Austria) environmental chamber attachment was integrated with a VTI Corporation (Hialeah, FL) RH-200 humidity generator.

Water Vapor Sorption/Desorption

Water sorption/desorption studies were conducted with a DVS-1000 dynamic vapor sorption system (Surface Measurement Systems, London, UK). The samples (10–20 mg) were initially dried at 40°C until a constant weight was achieved and then allowed to cool to 25°C. The RH was then increased from 0–90% in increments of 5%RH. Each successive increment was initiated manually when the change in sample mass at a given RH was less than 0.5 μg for 5 min.

Stability Study

Approximately 100 mg of each of the four powders (sodium indomethacin, lactose, raffinose, and sucrose) was aliquoted into several small glass vials. These vials were stored over saturated salt solutions in desiccators, which were placed in a temperature-controlled incubator at 25°C (VWR Corp., West Chester, PA, Model 1915). Each of the following salt solutions was used to provide an environment of a given RH at 25°C (23): LiBr (6.4%RH), LiCl (11.3%RH), LiI (17.6%RH), $KC_2H_3O_2$ (22.5%RH), KF (30.8%RH), K_2CO_3 (43.2%RH), and KI (68.9%RH). After exposure to the above conditions for at least 8 weeks, all powder samples were stored at < 2%RH to remove residual water as preparation for analysis by scanning electron microscopy (SEM) or BET surface area measurement.

Scanning Electron Microscopy

SEM was used to observe the morphology of the spray-dried particles before and after exposure to moisture. Samples were mounted on silicon wafers that were then mounted on top of double-sided carbon tape on an aluminum SEM stub. The mounted powders were then sputter-coated with gold:palladium in a Denton sputter-coater for 60 to 90 s at 75mTorr and 42mA. This produces a coating thickness of approximately 150Å. Images were taken with a Philips XL30 ESEM operated in high vacuum mode using an Everhart-Thornley detector to capture secondary electrons for the image composition. The accelerating voltage was set at 20kV using a LaB_6 source. The working distance was 5–6 mm.

BET Surface Area

The specific surface area of each spray-dried raffinose powder was determined by BET analysis of its nitrogen adsorption isotherm, as measured with a Quantachrome Autosorb-1C instrument (Quantachrome Instruments, Boynton Beach, FL). Approximately 200–400 mg of powder were placed in a glass sample tube. The sample was then purged with nitrogen gas for 16 h at 40°C to remove any residual water and any physically adsorbed material from the surface. Before each measurement, the filled sample tube was weighed to determine the sample mass, and it was then connected to the BET instrument. The tube was then immersed in a liquid nitrogen bath. The unoccupied volume was determined using helium gas. The relative pressures of nitrogen used were 0.050–0.300. For the samples with a specific surface area less than 1 m^2/g, krypton gas was used as the adsorbate.

To determine the specific surface area of each powder, the measured adsorption isotherm data were fit to the BET model to determine the amount of adsorbate (nitrogen or krypton) in an adsorbed monolayer. Based on the known molecular cross-sectional area of the adsorbate, the BET instrument's software calculated the surface area of the powder based on a linearized form of the BET isotherm equation.

RESULTS AND DISCUSSION

Features and Significance of the Moisture-Induced Thermal Activity Trace

Figures 1a–1d show results for isothermal (25°C) microcalorimetry experiments on spray-dried trehalose, sucrose, lactose, raffinose, and sodium indomethacin, respectively. In these experiments, samples were exposed to a nitrogen stream in which the RH was increased from 0–90%RH at 3%RH/hour. The measured power, abbreviated here as "MITAT" (moisture-induced thermal activity trace), is the total, nonspecific heat flux of interaction between the solid sample and water vapor. Figure 1 shows that the MITAT displays common features for all the spray-dried (amorphous) materials studied. Figure 1a shows that the MITAT is characterized by a low activity region, A; a ′take-off′ point, B; a high exothermic activity region, C; and an endothermic region, D.

Other workers have used isothermal microcalorimetry and other calorimetric techniques to obtain similar results to these (24–27). Here, we have used complementary characterization techniques to help interpret the various calorimetric

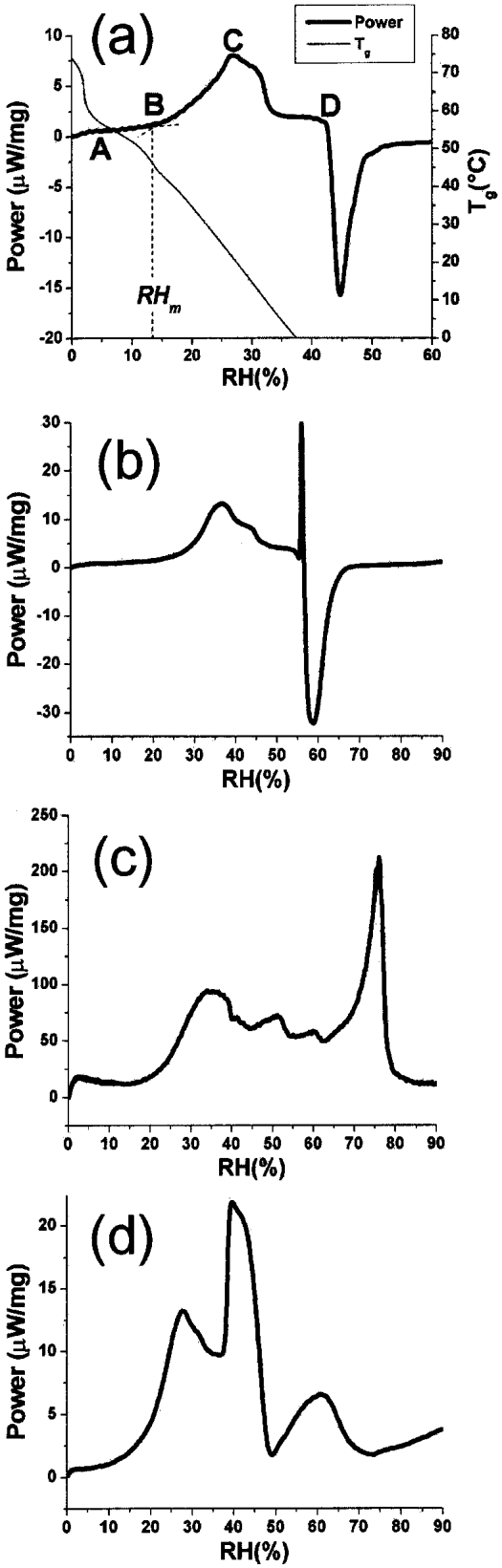

Fig. 1. (a) The moisture-induced thermal activity trace (MITAT) of sucrose at 25°C, showing regions of low thermal activity A (0<RH<13%), "take-off" point B ($RH_m \approx 13\%$), exothermic region C (13%<RH<27% = RH_p) and endothermic region D (RH>27%). MITATs at 25°C of: (b) lactose, (c) raffinose, and (d) sodium indomethacin.

events and to explain their relevance to solid-state physical stability. In this work, parallel experiments (MDSC, SEM, BET surface area, and XRPD) were performed to reveal the morphology and state of the solid in the various regions indicated in the MITAT. Results from SEM and XRPD analysis for sucrose are shown in Fig. 2. After 8 weeks of storage, SEM photomicrographs show that sucrose remains as discrete, amorphous particles in the low thermal activity region (A) and up to the take-off point (B). Therefore, the increase in rate at the take-off point is not due to geometrical changes in the sample but rather corresponds to an internal structural change. Slight structural collapse is observed after storage at an RH value slightly beyond the take-off point, 17.6%RH, even though the $T_g > T_{storage}$ (i.e., physical instability below T_g). Liquid bridges have formed, resulting in fusion between adjacent particles. Gross structural changes were observed after storage for 8 weeks at RH conditions corresponding to the maximum in the exothermic region (C), 31%RH. The lack of smooth, spherical particles indicates that crystallization has occurred throughout the sample. Crystallization has been confirmed by XRPD results (Fig. 2). Storage at higher RH values results in an increase in the size of crystals.

In Fig. 1, the heat flow signal decreases at RH values beyond C. We suspected that this decrease in the rate of sorption occurs because of a reduction in the specific surface area of the powder as it experiences structural collapse. To confirm this effect, we measured the specific surface areas of raffinose, as determined from BET analysis of nitrogen and krypton adsorption isotherms (Table I). For such a study, raffinose is a better model system than sucrose since it remains amorphous at RH values up to 43.2%RH. Because of this, structural collapse can be isolated from crystallization. Storage of amorphous raffinose at relative humidities beyond the first peak in the MITAT, RH_p, resulted in an irreversible reduction in its specific surface area.

Figure 1 also shows the T_g(RH) curve for sucrose/water mixtures, as predicted using the measured moisture sorption isotherm (wt% H_2O(RH)) and the best-fit of T_g data (28) using an equation of the Gordon-Taylor form. The T_g(RH) curve was developed using cubic spline fits of isotherm and T_g(wt% H_2O) data. The unusual shape of the curve is due to a mathematical combination of two nonlinear functions. We estimate that the uncertainty in our predicted T_g(RH) values is on the order of ±5°C. Table II shows the T_g at RH_p (for lactose, raffinose, sodium indomethacin, and sucrose), as predicted using the moisture sorption isotherm and T_g(wt% H_2O) data of each compound.

Just beyond RH_p, the T_g of the sample falls below the experimental temperature. However, the solid sample remains amorphous during the TAM experiment at relative humidities less than that at "D." At this point, crystallization begins to occur. Although crystallization is an exothermic process, it is manifested for many compounds as an endotherm in an RH-perfusion experiment. This occurs because water is liberated from the solid sample during crystallization, as is usually observed in gravimetric experiments (22,32,33). For an anhydrous crystal, its equilibrium moisture content (at a given RH) is less than the so-called "equilibrium" moisture content of the amorphous solid, and in general, the enthalpy of moisture desorption exceeds the enthalpy of crystallization. In contrast, formation of a hydrated crystal such as lactose monohydrate, raffinose pentahydrate, or sodium indo-

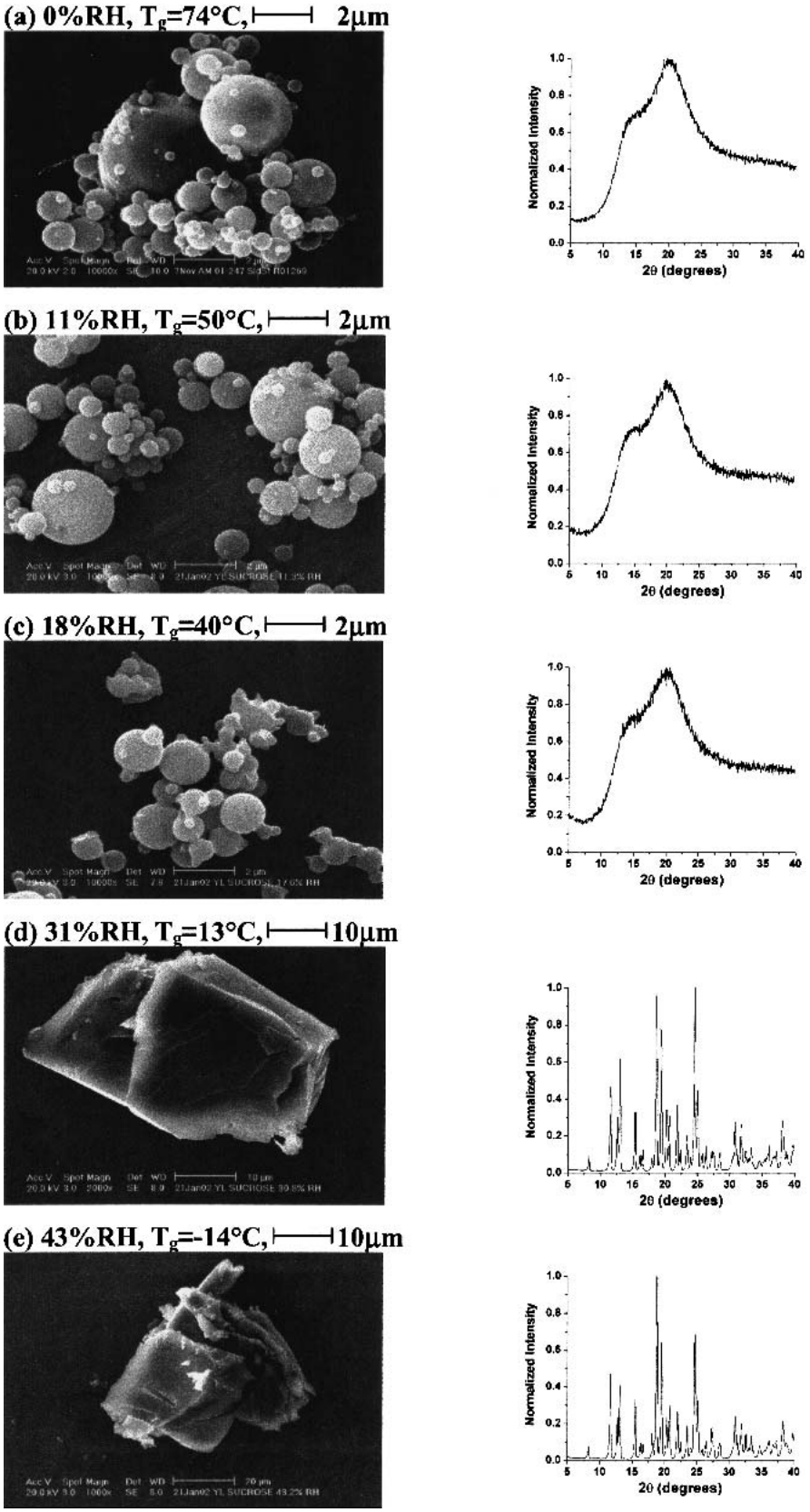

Fig. 2. Structural (XRPD) and morphologic (SEM) analyses of spray-dried sucrose at 25°C as a function of RH. SEM images and XRPD diffractograms are of powders stored at the indicated RH for 8 and 16 weeks, respectively. Particle fusion is observed at 17%RH; crystallization has occurred at and above 30.8%RH.

Table I. Specific Surface Area of Spray-Dried Raffinose following Eight Weeks of Storage at the Given Relative Humidities

RH at 25°C (%)	Specific surface area (m^2/g)
0.0%	3.9
17.6%	4.1
22.5%	3.8
30.8%	4.0
43.2%	9.3e-2
68.9%	1.7e-1

methacin tetrahydrate will be manifested as an exotherm when crystallization is not accompanied by water desorption (see Figs. 1b, 1c, and 1d, respectively) or when the enthalpy of desorption is small compared with the enthalpy of crystallization. Note that Fig. 1b shows a combination of the two behaviors: a narrow exotherm followed by a broad endotherm. We have found that in some cases, depending on the mass and geometry of the powder sample, lactose crystallization is manifested as a single endotherm. A gradient in the concentration of water in the powder can result in crystallization of a fraction of the lactose as lactose monohydrate. Upon further moisture sorption, the remaining sample also crystallizes as lactose monohydrate, resulting in desorption of excess water. To confirm such a hypothesis, complex processes such as simultaneous crystallization/desorption can be deconvoluted using hardware and software modifications, which will be discussed later in this report.

The "Take-Off" Point on the MITAT Behaves Like an RH Threshold

Here, we identify the RH at the take-off point as "RH_m". In practice, the take-off point is determined by linearly extrapolating data both below and above the initial bend in the power trace; RH_m lies at the intersection of these lines. At this point, changes are observed in the rate of moisture sorption without any apparent changes in the morphology of the glassy material (by SEM). An observation consistent with the long-term physical stability for RH<RH_m is that sucrose remained amorphous (according to XRPD) for more than 700 days when stored at 11.8%RH at 25°C (34). In contrast, sucrose crystallized within 200 days when stored at a slightly higher RH, 16.5% (34). In our laboratories, spray-dried amorphous sucrose, lactose, raffinose, and sodium indomethacin have remained amorphous (XRPD) and morphologically stable (SEM) for years when stored well below their RH_m values and for more than 8 weeks (at the time of submission of this manuscript) when stored just below their respective RH_m values (at 25°C).

Based on these properties of the MITAT take-off point, it is plausible to characterize RH_m as an RH threshold for molecular mobility. To further demonstrate that RH_m is an indicator of long-term stability, we used isothermal microcalorimetry to measure the time for the onset of crystallization of dry amorphous samples that were exposed to a humid environment. Using the TAM, a given dry, amorphous sample was subjected to a sudden step change in RH, and the heat flux was measured as a function of time. For each of several RH values (using a fresh sample in each case), the time to observe the calorimetric event indicative of crystallization was recorded. Results are shown in Fig. 3. Our measurements agree quite well with earlier work by Makower (34). The sample exposed to 15%RH remained amorphous for more than 5 days. At and below RH_m, the time necessary to observe crystallization exceeds the time scale of the experiment (about 5 days). Thus, crystallization was not observed.

Similar experiments were carried out with lactose and raffinose. Unlike sucrose, the observed onsets for crystallization converge not at RH_m but at higher RH values. It is likely that crystallization is delayed since at RH_m, there is insufficient water to form the stable crystalline forms, lactose monohydrate and raffinose pentahydrate. For example, lactose was observed to crystallize after 27 h when submitted to 30%RH but did not crystallize when stored for a week at 25%RH. The corresponding water contents from the equilibrium water sorption isotherm (25°C) are 3.8 and 5.2 wt% H_2O. (Lactose monohydrate contains 5wt% H_2O.) However, SEM photomicrographs of amorphous lactose exposed to 25%RH show signs of interparticle bridging, indicating high levels of molecular mobility.

Another type of step experiment can be used to gain more insight into the physical meaning and behavior of the take-off point. These experiments involved multiple sorption/desorption cycles in which the RH was increased, held constant, and then decreased in a stepwise fashion, as described in the "Methods" section. Figure 4 shows the results of such an experiment with sucrose, using step sizes of 5%RH, 10%RH and 15%RH. Based on the integrated areas of the peaks, two major conclusions can be drawn: Below 15%RH, the sorption/desorption process is entirely reversible, whereas above 15%RH, the sorption/desorption cycle is characterized by hysteresis. The hysteresis is qualitatively similar for all other compounds studied: The energy of sorption is greater than that for desorption. Hysteresis is due to either an irreversible physical change in the sample, or a change in the mode of water-vapor interaction with the amorphous sample.

The molar enthalpy of each RH step, ΔH, can be calculated from the total heat of interaction:

$$\Delta H = \frac{Q}{n} \tag{1}$$

where Q is the integral heat of adsorption in the MITAT for the given step, and n is the total moles of water absorbed, as given by the independently measured equilibrium moisture sorption isotherm (34). Figure 5 shows the calculated molar heats of interaction in increments of 3%RH. The heats of interaction at RH values beyond the MITAT take-off point are on the order of –40 kJ/mol, whereas the heat of condensation of water is –44 kJ/mole (25°C). We suggest that this agreement is a consequence of the mode of moisture sorption beyond RH_m, which is characterized by water-water interactions. Also, note that in all cases, the absolute values of the molar heats of interaction are less than the heat of condensation of pure water. Such behavior would be unusual for a purely sorptive process. However, sorption to the amorphous samples results in breakage of solid-solid hydrogen bonds, formation of water-solid bonds, and conformational changes in the solid. The sum of these processes is such that the overall energy of interaction is less than that for simple physisorption.

Table II. Water Content, W_m, and T_g at RH_m and RH_p Compared with the Water Content at the Calculated BET "Monolayer" (25°C)

Excipient	Water content at RH_m (RH_m (%RH))	Water content at RH_m (RH_m at RH_m[a] (wt %))	Dry T_g (this work) (°C)	T_g at W_m or RH_m (°C)	RH_p (%RH)	T_g at RH_p (°C)	BET W_o[b] (wt %)	GAB W_o (wt%)
Sucrose[c]	13	2.1	74	47	27	21	2.0 (fit 3 to 10.5% RH)	1.8 (fit 0–27% RH)
Raffinose[d]	17	3.3	113	70	36	38	4.7 (fit 5 to 30% RH)	3.6 (fit 0–50% RH)
Lactose[e]	16	2.5	110	83	43	44	2.9 (fit 0 to 20% RH)	1.8 (fit 5–30% RH)
Sodium indomethacin[f]	8	1.0	89	69	29	31	3.0 (fit 10 to 20% RH)	2.1 (fit 0–40% RH)

[a] Based on equilibrium moisture sorption isotherm at 25°C.
[b] From BET analyses of the moisture sorption isotherm at 25°C (only using data that fit the linearized form of the BET equation). T_g (wt% H_2O) predictions based on Gordon-Taylor regression of data in reference [c](28), [d](29), (30), and [e](31).
[f] Amorphous sodium indomethacin was prepared by spray-drying an equimolar mixture of indomethacin free acid and NaOH dissolved in methanol. This treatment likely resulted in a mixture of free acid and the sodium salt.

The results of the sorption/desorption step experiments and the heat of sorption measurements are consistent with the mechanism of a saturation process. The differences in the enthalpy and reversibility of sorption below and above RH_m suggest that RH_m delineates two distinct regimes of water-solid interactions. We hypothesize that W_m, the water content at RH_m, represents the solubility of water vapor in the solid matrix. This can be interpreted as the amorphous analogue to the deliquescence point of a crystalline material, RH_o. Beyond the solubility limit at RH_m, any additional absorbed water vapor behaves as a solvent for the amorphous matrix. In this view, the lack of energy hysteresis below RH_m suggests that water reversibly interacts with the amorphous solid. Slightly above RH_m, such a change in the interactions of the amorphous solid with water seems to facilitate the mobility of water even though the storage temperature is well below the T_g of the solid. Since the term "solubility" implies thermodynamic equilibrium, a more-accurate term to describe W_m is hydration limit, which involves interactions between the water molecules and the glassy solid.

These observations are consistent with results from nuclear magnetic resonance and high frequency Dielectric Resonance Spectroscopy measurements (8,10,35) of the chemical nature of the interactions between water and amorphous solids. Those studies suggest that the chemical environment of sorbed water molecules is different below and above the so-called "monolayer," as described by BET analysis of the measured moisture sorption isotherm. At water contents less than the hydration limit, the translational mobility of water is restricted in comparison with its mobility at water contents above the monolayer level (8). Table I shows that the moisture content at RH_m is commensurate with W_m determined from BET analyses of the moisture sorption isotherms. Table I also shows the calculated monolayer coverage based on analyses of the moisture sorption isotherms using an alternative sorption model, the GAB equation. Note that the calculated hydration limit depends on the model chosen. This model dependence provides further motivation to choose the calorimetric methodology presented here, since the MITAT can be measured and is necessarily model-independent.

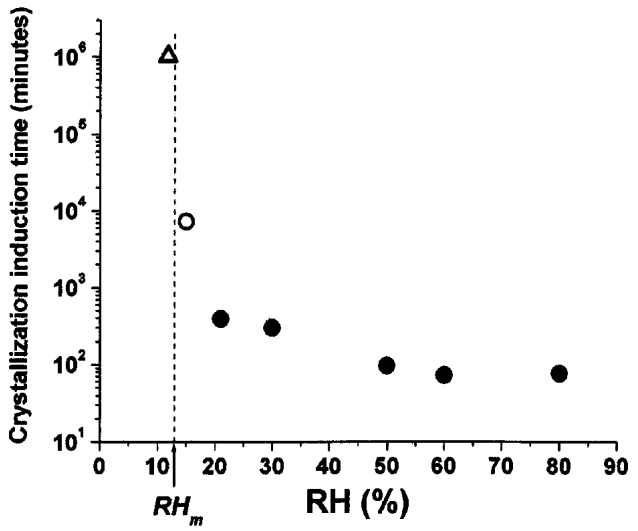

Fig. 3. The onset time for crystallization of spray-dried sucrose as a function of RH, as measured using TAM at 25°C. Independent samples (closed circles) were kept dry at constant temperature and then instantaneously exposed to the indicated RH. The open circle represents a lower limit since no crystallization was observed for 5 days at 15%RH. The open triangle is the datum reported by Makower and Dye (34) and represents a lower limit since they did not observe crystallization for 700 days at 25°C, as measured by XRPD and polarized light microscopy. The dashed line indicates the RH_m of amorphous sucrose at 25°C.

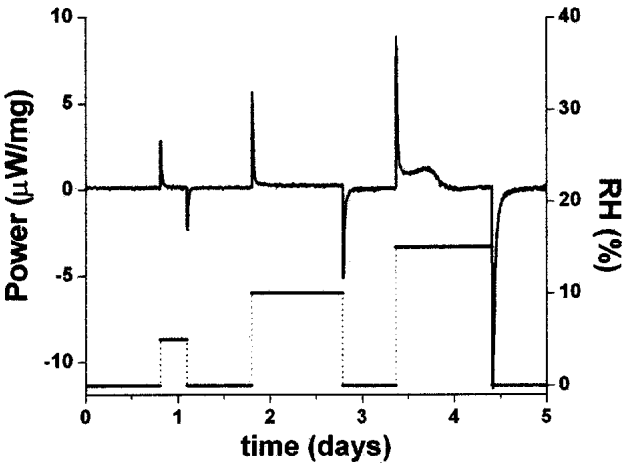

Fig. 4. Water vapor sorption/desorption cycles for sucrose, as measured using TAM at 25°C. Hysteresis is observed for the 15%RH step, which is above RH_m. (exothermic = upward).

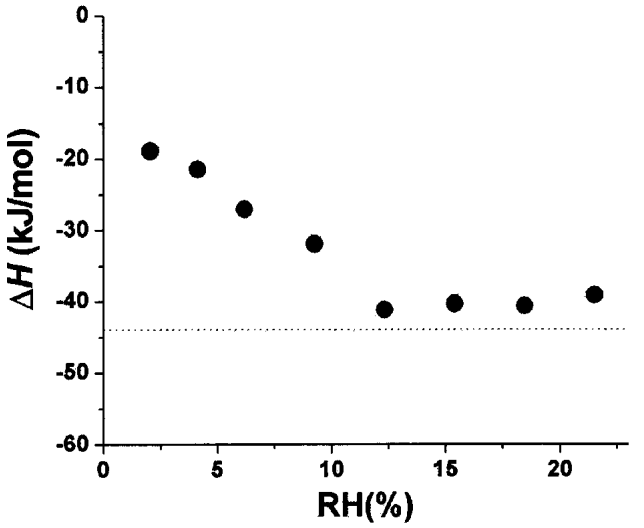

Fig. 5. The molar heat of water sorption of sucrose at 25°C. Reported values were calculated using Eq. 1. The dashed line indicates the latent heat of condensation of water at 25°C.

Furthermore, note that moisture sorption data for amorphous saccharides and many other organic glasses are not well described by the BET equation. For example, the BET model describes sucrose isotherm data only up to 12%RH. It has been suggested that under these conditions, this is due to water vapor *ab*sorption followed by dissolution of sucrose by water (36).

The Significance of the T_g at W_m

As W_g is associated with the amount of water to depress the T_g to the storage temperature, we were interested in the meaning of the T_g value associated with W_m, i.e., $T_g(W_m)$. The $T_g(W_m)$ values of the different compounds tested were determined from published results of the T_g dependence on water content. The $T_g(W_m)$ values were then compared with other available constants such as the so called "zero mobility temperature," T_o, which in many cases coincides with the Kauzmann temperature (37).

For sucrose, $T_g(W_m)\approx 47$°C. This was estimated based on W_m = 2.1wt% H_2O at 25°C, a dry T_g of 74°C, and a fitted Gordon-Taylor parameter of 0.1368 (31). Since the calorimetric experiment is performed at 25°C, $T_g(W_m)$-$T_{storage}$ = 22°C. For comparison, Shamblin *et al.* (2) reported that average relaxation times for sucrose exceed 3 years as long as it is kept below its T_o value of 48°C. Since they use the dry state as a reference, *dry* T_g–T_o = 26°C. Zhou *et al.* (37) also have determined a value of T_o for sucrose as 57°C with a reference temperature of 75°C, so *dry* T_g–T_o = 18°C.

For raffinose, the T_g at W_m (3.3 wt% H_2O) is 70°C, estimated using Gordon-Taylor parameters from (28). Hence, at 25°C, $T_g(W_m)$-$T_{storage}$ = 45°C. For comparison, Kajiwara *et al.* (3) reported a T_o of 65°C for dry raffinose, and the dry T_g of raffinose is about 113°C. Thus, *dry* T_g–T_o = 48°C.

For trehalose, the T_g at W_m (3.7 wt% H_2O) is 80°C (estimated from [38]). Hence, at 25°C, $T_g(W_m)$-$T_{storage}$ = 55°C. For comparison, Hatley (39) reported a T_o of 44°C for a sample of trehalose with a T_g of 101°C (containing 0.8% moisture), thus T_g–T_o = 56°C; in addition, Shamblin *et al.* (2) reported a T_o of 49°C for a sample with a T_g of 105°C, thus, T_g–T_o = 51°C.

Although the dry T_g (121°C) and the T_o for sodium indomethacin, 38°C, are available in the literature (40), the above analysis was not possible since our sample is a mixture of sodium indomethacin and free acid with a dry T_g of 89°C (based on the published T_g of acid/salt mixtures for indomethacin [41], our sample contains approximately 1:1 acid to salt molar ratio) and a $T_g(W_m)$ = 69°C.

In our view, this remarkable agreement in the required ΔT to observe long relaxation times suggests a connection between the state of water within the glassy solid and the average relaxation times measured by unrelated methodologies. Furthermore, our results provide support for a rapid, straightforward technique to estimate the combined effect of temperature and RH on the stability of amorphous solids. The effect of temperature will be the subject of a forthcoming research article.

Deconvolution of the MITAT

Standard calorimetric techniques are nonspecific. That is, they measure the total heat evolved or absorbed. Knowledge of the contribution of moisture sorption to the total measured heat signal adds valuable information toward understanding the behavior of these amorphous materials at the take-off point. DTIC experiments have been used to determine the individual energetic contributions of moisture sorption and desorption processes (21). In principle, these data can be used to construct the moisture sorption isotherm of the sample. This approach has been recently used by Lehto and Lain to study the water-induced crystallization of lactose and cefadoxil (27).

The amount of moisture sorbed can then be used to calculate the heat flux due only to moisture sorption/desorption (22). The difference between the total measured heat flux in the sample calorimeter and that calculated using the RH_{out} data is the heat flux due to all processes other than moisture sorption (i.e., structural collapse, crystallization, enthalpic relaxation, etc.). Thus, using this technique, the heat flux signal can be readily deconvoluted into contributions due to moisture sorption/desorption and those due to other energetic processes.

The above analysis assumes that the heat of interaction between the amorphous solid and water vapor is the same as the heat of condensation of water at atmospheric pressure. Studies of sorption of numerous polar and nonpolar molecules on carbon black show that this is a reasonable assumption at sorption levels beyond the hydration limit (42). Near the hydration limit, the isosteric enthalpy of adsorption was found to approach the heat of liquefaction. Figure 5 and Table III demonstrate that for sucrose at RH > 15%, this is a reasonable approximation.

As an example of this deconvolution technique, Fig. 6 shows the dissection of the measured heat flux of sucrose at 25°C into the calculated heat flux due to water sorption and that due to all other energetic processes that do not involve sorption or desorption of water. It is clear that most of the first region (A), take-off point (B), and region (C) can be explained solely by moisture sorption. It is only at the end of the exothermic region (D) that other processes become prominent and may be related to the water-induced collapse of the glassy phase as supported by the decrease of surface area.

Table III. Molar Heat of Interaction of Spray-Dried Sucrose and Water Vapor at 25°C Calculated from the Total Heat of Sorption and the Equilibrium Moisture Sorption Isotherm

RH (corrected) (%)	[a]Q (J/g sucrose)	[b]W_{eq} (wt%)	ΔH_{abs} (kJ/mol H_2O)
5.15	–5.9	1.26	–8.33
10.3	–17.1	1.87	–16.2
15.4	–58.5	2.48	–41.4
20.5	–72.5	3.27	–38.6
25.6	–96.7	4.52	–36.8

[a] From isothermal microcalorimetry experiment at 25°C.
[b] From dynamic vapor sorption measurements of the equilibrium moisture sorption isotherm at 25°C.

Interestingly, the RH of the outgoing nitrogen stream is independent of the RH of the incoming nitrogen stream from the take-off point B to approximately the peak in the MITAT, point C, at which the sample T_g is roughly the experimental temperature. This behavior is similar to that found for a saturated salt solution, where the water activity remains constant as long as there is solid phase to be dissolved.

The crystallization event, shown as an endotherm in the sucrose MITAT, involves the concomitant evaporation of water. The evaporation process is readily apparent by the sudden increase in RH_{out}. Subtraction of the heat flux due to moisture sorption/desorption from the total heat flux reveals the underlying exotherm of crystallization. This analysis demonstrates that the use of DTIC combined with the GPCD adds specificity to the MITAT and is a powerful tool for interpretation of observed, and often complex, superimposed energetic events.

Other authors have noted the smooth trend between the equilibrium vapor pressure over aqueous sucrose solutions and that over low-moisture amorphous sucrose (34,36). These data describe the water-rich and water-poor regimes, respectively. Although the intermediate region is not experimentally accessible because of crystallization of sucrose, it is tempting to treat the low moisture compositions as supersaturated aqueous solutions. Carstensen and Van Scoik (36) have shown that the calculated BET monolayer of sucrose based on sorption of water is about two orders of magnitude greater than that calculated from nitrogen adsorption. This suggests that water is predominantly absorbed to sucrose, a view supported by the ability of solution theories to describe the behavior of these seemingly solid samples (11,43). Adopting this view, a hypothetical process can be constructed to describe the events that occur as an increasing amount of water becomes associated with sucrose, as happens during a RH-perfusion calorimetry experiment. In practice, water vapor is adsorbed/absorbed to the saccharide. At some water content, the amorphous solute begins to dissolve, and an aqueous solution is formed. A thermodynamic pathway can be constructed from two distinct steps, as described by the following equation:

$$Q = \left(\frac{m_w}{MW_w}\right)\Delta H^{vap} + \Delta H^{sol}(x_w) \qquad (2)$$

where Q is the heat liberated per gram of sucrose, m_w is the mass of water sorbed per gram of sucrose, MW_w is its molecular weight (18.016 g/mol), ΔH^{vap} is the molar enthalpy of condensation of water at 25°C (-44 kJ/mol), and $\Delta H^{sol}(x_w)$ is the heat of solution for dissolution of 1 g of pure amorphous sucrose to a final sucrose mass fraction x_w. The first term of Eq. 2 describes the condensation of water vapor. In the second step, this liquid water is mixed with the solute to form a supersaturated solution. Heat of solution and dilution data are generally unavailable. However, Culp has published such data over the entire range of sucrose/water compositions (44). Thus, from knowledge of the amount of moisture sorbed, the total heat of this hypothetical condensation/mixing process can be calculated using Eq. 2. This can be compared with the heat determined in an RH step experiment or the heat from integration of the TAM power-time trace of an RH ramp experiment. Figure 7 compares the calculated heat with that measured calorimetrically. Such an analysis provides some

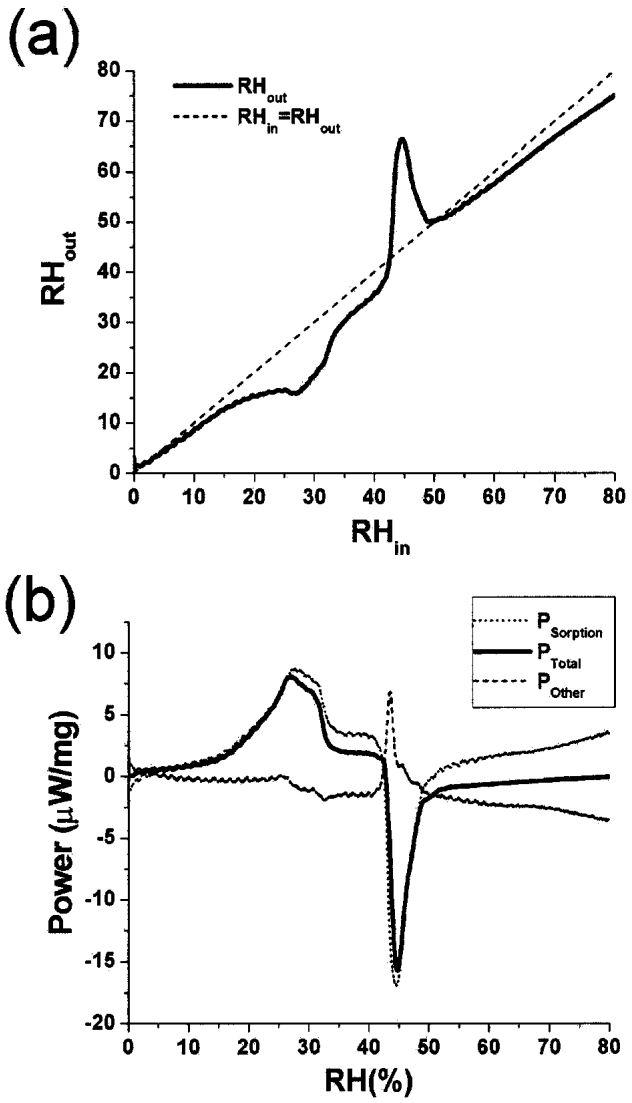

Fig. 6. Deconvolution of the MITAT of spray-dried sucrose: (a) Deviation between the RH_{in} (dashed line) and the calculated RH_{out} (solid line) values indicates processes in which water is sorbed or liberated, such as crystallization. (b) MITAT of spray-dried sucrose at 25°C (thick line), showing the calculated heat flux due to moisture sorption (thin line). The collective heat flux due to all other events (i.e., structural relaxation, collapse, and crystallization) is defined as $P_{other} = P_{Total} - P_{Sorption}$. (dashed trace).

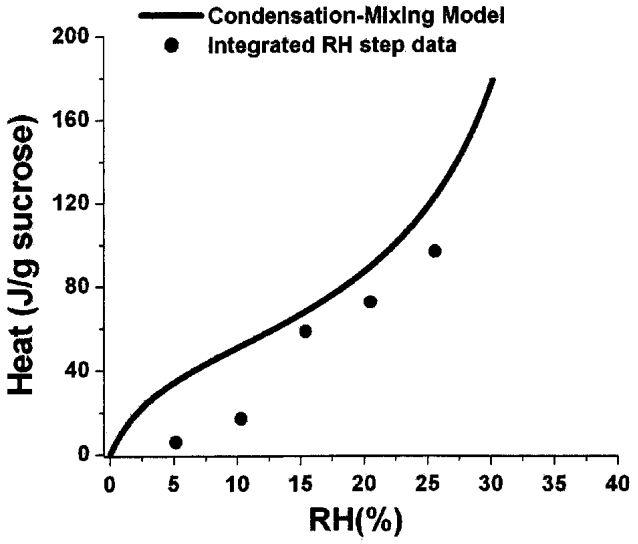

Fig. 7. Comparison of integral heats of interaction at 25°C with those predicted using a two-step condensation-mixing model (Eq. 2).

insight into the interaction of water vapor with the amorphous solid. At low RH values, the heat of sorption is typically less exothermic than the heat of condensation of water. Thus, the hypothetical model deviates from what is actually measured. However, at some point, the behavior of the system becomes more solution-like, and the above hypothetical process approaches that which is measured calorimetrically. For sucrose, this occurs at about 15%RH, a value that is consistent with RH_m.

CONCLUSIONS

We have used isothermal microcalorimetry to measure the MITAT, which shows general behavior for the spray-dried amorphous compounds of this study. Analysis of the MITAT yields information about the mode of interaction between water vapor and the amorphous solid. This technique provides a direct measurement of RH_m, which delineates a change in water-solid interactions. The good agreement between RH_m and our physical stability measurements, reinforced with literature data on long-term physical stability, provides support for RH_m as a meaningful indicator of stability.

Below RH_m (or W_m), moisture sorption is reversible, as demonstrated by the absence of energy hysteresis. This is supported by measurements of the specific surface area of an amorphous material after a complete sorption/desorption cycle below RH_m. Absence of hysteresis in the energy of interaction is an indication of long relaxation times. Above RH_m (or W_m), changes are observed in the energy of interaction and rates of water absorption. These observations are consistent with literature studies suggesting that the chemical environment of water molecules is different below and above the hydration limit.

We proposed that RH_m is analogous to the RH to induce deliquescence of a crystalline solid, RH_o. This mechanism proposes that at RH_m, water vapor saturates binding sites within the amorphous phase. Above RH_m, water becomes the solvent and the system behaves like a supersaturated solution. This water-binding site saturation process is supported by calorimetric measurements showing that above RH_m, the heat of water sorption approaches the enthalpy of condensation of water. Above RH_m, the good agreement of calorimetric data with a simple condensation/mixing model further illustrates this point. In addition, the RH of the outgoing nitrogen stream, in the DTIC experiments, is independent of the RH of the incoming nitrogen stream from the take-off point B to approximately the peak in the MITAT, point C, at which the sample T_g is roughly the experimental temperature. This behavior is similar to that found for a saturated salt solution, where the water activity remains constant as long as there is solid phase to be dissolved.

Furthermore, for each compound in this study, the water content at RH_m, W_m, is in good agreement with the monolayer value determined from BET analysis of the water sorption isotherm. The T_g at W_m seems to correspond to a threshold temperature, T_o, for long-term stability, which characterizes the molecular mobility of water within the hydrated glassy solid. Undoubtedly, the MITAT offers insight on the molecular state of water within the hydrated glassy solid, which previously could be accessed only by spectroscopic means.

Finally, DTIC is a powerful technique to further elucidate the conditions under which to expect stability of common amorphous pharmaceutical excipients. Deconvolution of superimposed energetic processes adds specificity to isothermal microcalorimetry.

ACKNOWLEDGMENTS

The authors gratefully acknowledge our colleagues from Nektar Therapeutics (formerly Inhale Therapeutics, Inc.), Trixie Tan and Lisa Williams, for much of the experimental work presented here; Alex Mandel and Yi Liang for the SEM images; and Kathy Farinas, Jayne Hastedt, and Sarma Duddu for helpful discussions and insight provided throughout this work. DLB dedicates this work to Cecilia Espadas and thanks her for her unfailing love and faithful support, and for taking care of the boys (David Alberto and Luis Daniel). Aziz Bakri thanks Dr. J. Suurkuusk of Thermometric AB for his continued interest in the development of the prototype of the DTIC and GPCD. Further information regarding the DTIC or French references can be obtained by contacting Aziz Bakri (Aziz.Bakri@ujf-grenoble.fr).

REFERENCES

1. S. P. Duddu and T. D. Sokoloski. Dielectric analysis in the characterization of amorphous pharmaceutical solids. 1. Molecular mobility in poly(vinylpyrrolidone)—water systems in the glassy state. *J. Pharm. Sci.* **84**:773–776 (1995).
2. S. L. Shamblin, X. Tang, L. Chang, B. C. Hancock, and M. J. Pikal. Characterization of the time scales of molecular motion in pharmaceutically important glasses. *J. Phys. Chem. B* **103**:4113–4121 (1999).
3. K. Kajiwara, F. Franks, P. Echlin, and A. L. Greer. Structural and dynamic properties of crystalline and amorphous phases in raffinose-water mixtures. *Pharm. Res.* **16**:1441–1448 (1999).
4. V. Andronis and G. Zografi. The molecular mobility of supercooled amorphous indomethacin as a function of temperature and relative humidity. *Pharm. Res.* **15**:835–842 (1998).
5. B. J. Aldous, F. Franks, and A. L. Greer. Diffusion of water within an amorphous carbohydrate. *J. Mater. Sci.* **32**:301–308 (1997).
6. R. Pethig. Protein-water interactions determined by dielectric methods. *Ann. Rev. Phys. Chem.* **43**:177–205 (1992).

7. S. Yoshioka, Y. Aso, and S. Kojima. The effect of excipients on the molecular mobility of lyophilized formulations, as measured by glass transition temperature and NMR relaxation-based critical mobility temperature. *Pharm. Res.* **16**:135–140 (1999).
8. C. A. Oksanen and G. Zografi. Molecular mobility in mixtures of absorbed water and solid poly(vinylpyrrolidone). *Pharm. Res.* **10**: 791–799 (1993).
9. L. S. Taylor, F. W. Langkilde, and G. Zografi. Fourier transform Raman spectroscopic study of the interactions of water vapor with amorphous polymers. *J. Pharm. Sci.* **90**:888–901 (2001).
10. S. Bone. Dielectric and gravimetric studies of water binding to lysozyme. *Phys. Med. Biol.* **41**:1265–1275 (1996).
11. B. C. Hancock and G. Zografi. The use of solution theories for predicting water vapor absorption by amorphous pharmaceutical solids: A test of the Flory-Hoggins and Vrentas Models. *Pharm. Res.* **10**:1262–1267 (1993).
12. T. P. Labuza. The effect of water activity on reaction kinetics of food deterioration. *Food Tech.* **34**:36–41, 59 (1980).
13. M. J. Pikal, K. Dellerman, and M. L. Roy. Formulation and stability of freeze-dried proteins: Effects of moisture and oxygen on the stability of freeze-dried formulations of human growth hormone. *Pharm. Res.* **8**:427–436 (1991).
14. M. J. Hageman, P. L. Possert, and J. M. Bauer. Prediction and characterization of the water sorption isotherm for bovine somatotropin. *J. Ag. Food Chem.* **40**:342–347 (1992).
15. H. R. Costantino, J. G. Curley, and C. C. Hsu. Determining the water sorption monolayer of lyophilized pharmaceutical proteins. *J. Pharm. Sci.* **86**:1390–1393 (1997).
16. M. J. Hageman. The role of moisture in protein stability. *Drug Dev. Ind. Pharm.* **14**:2047–2070 (1988).
17. R. Huettenrauch and J. Jacob. Uber einen neuen Zusammenthang Zwischen Tablettenbildung und Feuchtigkeit der Ausgangsstoffe. *Pharmazie* **32**:241–242 (1977).
18. M. J. Kontny and C. A. Mulski. Gelatin capsule brittleness as a function of relative humidity at room temperature. *Int. J. Pharm.* **54**:79–85 (1989).
19. A. Bakri. Design, testing and pharmaceutical applications of a gas pressure controller device for solid-gas microcalorimetric titration. Application Note 22021, Thermometric AB, Sweden, 1993 pp. 4.
20. A. Bakri. Utilisation de la microcalorimétrie isotherme dans la formulation des formes pharmaceutiques solides, 1ères Rencontres Galéniques de Rabat; Le Comprimé demain Rabat, Morocco, 1994 pp. 137–151.
21. A. Bakri. Calorimetric powder characterization: A new calorimetric-sensitive method for simultaneous determination of sorption isotherms, surface energies, and physical/chemical reactivity of powders, *Problem Solving Using Calorimetric Methods*, Royal Society of Chemistry, London, 1995.
22. A. Bakri. A novel calorimetric approach to the study of interactions between gases and materials, 25th North American Thermal Analysis Society, pp. 3–10, Omnipress, McLean, Virginia, 1997.
23. L. Greenspan. Humidity fixed points of binary saturated aqueous solutions. *J. Res. Natl. Bur. Stand. Sec. A* **81**:89–102 (1977).
24. M. Angberg, C. Nystrom, and S. Castensson. Evaluation of heat-conduction microcalorimetry in pharmaceutical stability studies. VI. Continuous monitoring of the interaction of water vapor with powders and powder mixtures at various relative humidities. *Int. J. Pharm.* **83**:11–23 (1992).
25. L. D. Hansen, M. T. Pyne, and R. W. Wood. Water vapor sorption by cephalosporins and penicillins. *Int. J. Pharm.* **137**:1–9 (1996).
26. L. D. Hansen, M. T. Pyne, and R. W. Woo. Calorimetric method for rapid determination of critical water vapor pressure and kinetics of water sorption on hygroscopic compounds. *Int. J. Pharm.* **135**:31–42 (1996).
27. V.-P. Lehto and E. Lain. Simultaneous determination of the heat and quantity of vapor sorption using a novel calorimetric method. *Pharm. Res.* **17**:701–706 (2000).
28. A. Saleki-Gerhardt and G. Zografi. Non-isothermal and isothermal crystallization of sucrose from the amorphous state. *Pharm. Res.* **11**:1166–1173 (1994).
29. A. Saleki-Gerhardt, J. G. Stowell, S. R. Byrn, and G. Zografi. Hydration and dehydration of crystalline and amorphous forms of raffinose. *J. Pharm. Sci.* **84**:318–323 (1995).
30. K. Kajiwara and F. Franks. Crystalline and amorphous phases in the binary system water-raffinose. *J. Chem. Soc. Faraday Trans.* **93**:1779–1783 (1997).
31. B. C. Hancock and G. Zografi. The relationship between the glass transition temperature and the water content of amorphous pharmaceutical solids. *Pharm. Res.* **2**:471–477 (1994).
32. A. Saleki-Gerhardt, C. Ahlneck, and G. Zografi. Assessment of disorder in crystalline solids. *Int. J. Pharm.* **101**:237–247 (1994).
33. G. Buckton and P. Darcy. The use of gravimetric studies to assess the degree of crystallinity of predominantly crystalline powders. *Int. J. Pharm.* **123**:265–271 (1995).
34. B. Makower and W. B. Dye. Equilibrium moisture content and crystallization of amorphous sucrose and glucose. *Agr. Food Chem.* **4**:72–77 (1956).
35. M. Karel. Recent research and development in the field of low-moisture and intermediate-moisture foods. *CRC Crit. Rev. Food Technol.* **3**:329–373 (1973).
36. J. T. Carstensen and V. Scoik. Amorphous to crystalline transformation of sucrose. *Pharm. Res.* **7**:1278–1281 (1990).
37. D. Zhou, G. G. Z. Zhang, D. Law, D. J. W. Grant, and E. A. Schmitt. Physical stability of amorphous pharmaceuticals: Importance of configurational thermodynamic quantities and molecular mobility. *J. Pharm. Sci.* **91**:1863–1872 (2002).
38. D. P. Miller, J. J. de Pablo, and H. Corti. Thermophysical properties of trehalose and its concentrated aqueous solutions. *Pharm. Res.* **14**:578–589 (1997).
39. R. H. M. Hatley. Glass fragility and the stability of pharmaceutical preparations—Excipient selection. *Pharm. Dev. Tech.* **2**:257–264 (1997).
40. P. Tong and G. Zografi. Solid-state characteristics of amorphous sodium indomethacin relative to its free acid. *Pharm. Res.* **16**: 1186–1192 (1999).
41. P. Tong and G. Zografi. A study of amorphous molecular dispersions of indomethacin and its sodium salt. *J. Pharm. Sci.* **90**: 1991–2004 (2001).
42. R. A. Beebe, J. Biscoe, W. R. Smith, and C. B. Wendell. Heats of adsorption on carbon black. II. *J. Am. Chem. Soc.* **69**:2294–2299 (1948).
43. J. Zhang and G. Zografi. The relationship between the BET and structural relaxation models for water vapor sorption into amorphous solids. *J. Pharm. Sci.* **89**:1063–1071 (2000).
44. E. J. Culp. Heat of solution: Sucrose in water. *Sugar* **41**:44–46 (1946).